General Disclaimer

One or more of the Following Statements may affect this Document

- This document has been reproduced from the best copy furnished by the organizational source. It is being released in the interest of making available as much information as possible.

- This document may contain data, which exceeds the sheet parameters. It was furnished in this condition by the organizational source and is the best copy available.

- This document may contain tone-on-tone or color graphs, charts and/or pictures, which have been reproduced in black and white.

- This document is paginated as submitted by the original source.

- Portions of this document are not fully legible due to the historical nature of some of the material. However, it is the best reproduction available from the original submission.

NASA

Technical Memorandum 82070

INTERPRETATION OF COSMIC RAY COMPOSITION : THE PATHLENGTH DISTRIBUTION

R.J.Protheroe, J.F.Ormes
and G.M.Comstock

JANUARY 1981

Interpretation of Cosmic Ray Composition:

The Pathlength Distribution

R. J. Protheroe,* J. F. Ormes and G. M. Comstock**

Laboratory for High Energy Astrophysics
NASA/Goddard Space Flight Center
Greenbelt, MD 20771

ABSTRACT

The chemical composition of cosmic ray nuclei with $3 \leq Z \leq 28$ between a few hundred MeV/nuc and a few hundred GeV/nuc are compared with a consistent set of propagation calculations. These include the effects of spallation (energy-dependent cross sections are used), escape, ionization loss in the interstellar medium and deceleration in the solar cavity. The amount of matter traversed by cosmic rays is found to be about 7 g/cm^2, independent of energy between 100 MeV/nuc and 2 GeV/nuc. Above 2 GeV/nuc, the escape length varies as $E^{-0.4\pm0.1}$. In addition, a procedure has been developed to measure the shape of the cosmic ray pathlength distribution.

Utilizing the ratio of Fe-secondaries to Fe in the cosmic rays, presently available data are found to be consistent with an exponential distribution, and to eliminate models in which the path length distribution is severely truncated. To tie down the shape of the distribution more precisely, new measurements of the cosmic ray composition presently becoming available from experiments on the HEAO-3 satellite will have to be coupled with improved measurements of the energy dependence of partial and total cross sections.

Subject Headings: cosmic rays: abundances—interstellar: matter

* NAS/NRC Resident Research Associate.
**Cosmo-Science Associates, Stony Brook, NY

Introduction

The chemical composition of cosmic rays reflects information not only
on the mean amount of matter traversed by the particles between their sources
and the solar system, but also on the shape of the distribution of matter as
sampled by the particles. As is well known, cosmic ray nuclei from sources
(primaries) spall on traversing the matter in interstellar space, producing
secondary nuclides. By studying the relative composition of heavier
secondary nuclides which are rare or absent at the source, the shape (or
moments) of the path length distribution can be studied. This shape reflects
the location (either spatially or temporally) o' sources relative to the
observer (Owens, 1976), and hence is important .n understanding their origin.

In this paper we present calculations of t e effects of the distribution
of path lengths through which the cosmic rays p 'opagate on the detailed
chemical composition and compare these calculat .ons with data from a variety
of experiments ranging from 100 MeV/nuc to 100 ;eV/nuc.

It has been generally believed that the co position was best explained
by a path length distribution (PLD) with an abs ance of short path lengths.
This was thought necessary to explain the large number of nuclei observed in
the sub-iron region (Shapiro and Silberberg, 19/0; Shapiro, Silberberg and
Tsao, 1973; Garcia-Munoz and Simpson, 1970; Fic itel and Reames, 1968). Since
that time new measurements have been made of so ne of the cross sections
involved. The mean matter traversed has been found to vary with energy, and
more accurate charge composition measurements h ive been made.

There is a sound theoretical basis for a P .D in which short path lengths
are absent. Lezniak and Webber (1979) have derived the PLD shapes expected
in some of these models. In one such model som i of the matter through which
cosmic rays pass is located in the cosmic ray s urce. Cowsik and Wilson
(1973, 1975) first invoked a "double or nested leaky box" model to explain the

early observations of energy dependent changes in the abundance ratios of primary cosmic rays. Simon (1977) introduced a convenient parameterization of the PLD resulting from these models in terms of the convolution of two exponential distributions. We utilize this formalism to investigate the shape of the PLD using the cosmic ray data.

In this paper, the available data will be compared with a self consistent set of calculations. By comparing the data from different groups with the same model, any differences which might exist between calculations are eliminated in interpreting the data.

We will assume that acceleration of cosmic rays during their propagation in the interstellar medium is negligible and that the cosmic rays are effectively injected into the galaxy with a power law spectrum common to all species. This would apply if cosmic rays are accelerated in localized accelerators and then injected into the interstellar medium where the probability of subsequent acceleration is small. This could be localized shocks (Blandford and Ostriker, 1978; Jokipii and Higdon, 1979), the acceleration of a thermal plasma to cosmic ray energies (Eichler, 1980) or acceleration in supernova remnants (Scott and Chevalier, 1975).

We begin with the simple leaky box model (Cowsik et al. 1967), a model of cosmic ray propagation in which the PLD is exponential. Using the observed relative abundance of the light secondary elements Be and B and the primary elements C and O, we can determine a mean escape length $\lambda_e(E)$ as a function of energy. The general features found by Ormes and Freier (1978) are present: a decreasing escape length at high energies (> 2 GeV/nuc), and a constant escape length at lower energies. Jones (1979) has shown that the general shape of $\lambda_e(E)$ can be explained by a galactic wind model (Jokipii, 1976) in which escape of particles by diffusion dominates at high energies while escape by convection dominates at low energy.

The effect of varying the shape of the PLD on the secondary nuclei in the range 21<Z<25 just below the abundant primary iron nuclei is studied since the abundance of these elements is more sensitive to the shape of the PLD than the light secondary elements. Such studies are dependent upon a knowledge of the partial cross sections for producing each secondary isotope from every possible primary isotope. Insufficient measurements of the energy dependence of these important cross sections have been made as noted by Raisbeck (1979) and care must therefore be taken when using these data. We use here the semi-empirical formulations of Silberberg and Tsao (1973, 1973a, 1977, 1977a, 1977b, and Tsao and Silberberg, 1979) including all their corrections based upon the recent measurements with the Bevalac. The various versions of these formulations have been cross checked with Silberberg and Tsao under a community-wide effort initiated by P. S. Freier. We shall discuss the limitations on the interpretations due to uncertainties in the cross sections.

Method of Calculation

In the equilibrium steady-state homogeneous model, the intensity $J_i(E)$ of particles of type i at energy E is given by

$$Q_i(E) - \frac{J_i(E)}{\lambda_e^i(E)} - \frac{J_i(E)}{\lambda_{dec}^i(E)} - \frac{J_i(E)}{\lambda_{int}^i(E)} + \sum_{k \geq i} \left\{ \frac{J_k(E)}{\lambda_{spall}^{ki}(E)} \right.$$

$$\left. + \frac{J_k(E)}{\lambda_{dec}^{ki}(E)} \right\} - \frac{d}{dE} [w_i(E)J_i(E)] = 0 \qquad (1)$$

where Q_i is the source term; λ_e^i, λ_{dec}^i and λ_{int}^i are the mean path lengths for escape, decay and interaction of nuclei of species i; λ_{spall}^{ki} and λ_{dec}^{ki} are the mean path length for spallation and decay of nuclei of species k into species i; $-w_i(E)$ is the mean energy loss per unit path length. Note that $\lambda_{int \atop (spall)} = \frac{<m>}{\sigma_{int \atop (spall)}}$, and $\lambda_{dec} = \gamma\tau_{dec}\beta cn<m>$, where n and $<m>$ are the mean number density and mass of interstellar nuclei encountered by the cosmic rays, taken to be 0.3 cm^{-3} and 1.3 amu, respectively.

In actual calculations, solutions $J_i^S(E,x)$ to the slab model equations,

$$\frac{\partial J_i^S(E,x)}{\partial x} + \frac{J_i^S(E,x)}{\lambda_{dec}^i(E)} + \frac{J_i^S(E,x)}{\lambda_{int}^i(E)} - \sum_{k>i} \left\{ \frac{J_k^S(E,x)}{\lambda_{spall}^{ki}(E)} + \frac{J_k^S(E,x)}{\lambda_{dec}^{ki}(E)} \right\}$$

$$+ \frac{d}{dE}[w_i(E)J_i^S(E,x)] = 0 . \tag{2}$$

with initial conditions, $J_i^S(E,0) = Q_i(E)$, may be obtained numerically:

$$J_i^S(E,x) = J_i^S(E_i,x-\Delta x) \frac{w_i(E_i)}{w_i(E)} \left\{ 1 - \frac{\Delta x}{\lambda_{int}^i(E)} - \frac{\Delta x}{\lambda_{dec}^i(E)} \right\}$$

$$+ \sum_{k>i} \frac{w_k(E_k)}{w_k(E)} J_k^S(E_k,x-\Delta x) \left\{ \frac{\Delta x}{\lambda_{spall}^{ki}(E)} + \frac{\Delta x}{\lambda_{dec}^{ki}(E)} \right\} \tag{3}$$

Here E_i is the energy of a nucleus of species i at pathlength $(x-\Delta x)$ such that its energy at pathlength x is E. E_i is obtained from range-energy tables or, for small relative losses in energy, $E_i \cong E - w_i(E)\Delta x$.

The solutions $J_i(E)$ to the full equation may then be obtained from $J_i^S(E,x)$ by weighting with the pathlength distributions $P_i(x,E)$ (e.g. Lezniak, 1979):

$$J_i(E) = \int_0^\infty J_i^S(E,x)P_i(x,E)dx \tag{4}$$

For an exponential PLD, $P_i(x,E) = \exp\{-x/\lambda_e^i(E)\}$. For cross checking purposes, when using an exponential pathlength distribution, we can include an additional term $-\Delta x/\lambda_e^i(E)$ within the first curly bracket of equation (3) and use $P_i(x,E) = 1$ in equation (4).

For the spallation cross sections, we have used the Silberberg and Tsao semi-empirical formulae and taken an interstellar medium consisting of 90 percent hydrogen and 10 percent helium by number. Some of the important cross sections at just a few of the energies used in our calculation for the spallation of ^{12}C and Fe are given in Tables 1 and 2. These

cross sections include the effects of the decay of isotopes with half lives less than 10^{13}s and should thus be considered the "cosmic ray cross sections." In each case the cross section given is in mb per average interstellar nucleus and for Table 2 the cross sections have also been weighted with the expected abundances of Fe isotopes in the cosmic radiation. These tables illustrate the importance of using the observed energy dependence of the cross sections; e.g., the cross section for production of Cr by spallation of Fe varies by a factor of 4 between 100 MeV/nuc and high energies. Any error in the spallation cross sections will be directly reflected as an error in that predicted secondary-to-primary ratio.

Ionization losses are also very important in determing cosmic ray spectra at low energies and cannot be ignored. The effects of neglecting the energy dependence of the spallation cross sections and of neglecting ionization losses on the ratios of Fe-secondaries to Fe and (Be+B) to C are illustrated in Figure 1 (for the model we adopt as our "standard" to be described later).

The total cross sections adopted also affect the predicted composition, particularly for heavy nuclei (e.g., sub-Fe/Fe ratio) where particle losses are dominated by nuclear interaction rather than escape. We use the energy independent fits to the data obtained by Hagen (1976):

$$\sigma_{int} = 10\pi(1.29)^2[A_T^{1/3}+A_B^{1/3} - 1.189 \exp\{-0.05446 \min(A_T, A_B)\}]^2 \text{ mb} \quad (5)$$

where A_T and A_B are the mass numbers of the target nuclei (interstellar matter) and the beam (cosmic ray nuclei). An energy dependent total cross section scaled from the (p, p) cross section (Karol, 1975) has been used by Garcia-Munoz et al. (1979) in their analysis. While perhaps theoretically justified, the present data are unable to determine the energy dependence with any certainty and new measurements are urgently needed. The values used here (e.g., 716 mb for the p-Fe total inelastic cross section) may be somewhat low. Values in the literature range from 721 ± 7 mb (Roberts et al. 1979) to 779 ± 27 mb (MacFall et al., 1979) for measurements at energies above 100 GeV, but the inelastic cross

section rises with energy. The former cross section is an n-Fe measurement and the latter a p-Fe measurement. What is needed in our calculations is the mass changing cross section (taking account of Fe → Fe + n) and the only measurement is 750 ± 50 mb (Westfall et al., 1979). Our adoption of the Karol (1975) energy dependent form would reduce our predicted Sub-Fe to Fe ratio by about 10 percent above 400 MeV for the same grammage.

In our calculations we use the elemental source composition derived by Lezniak and Webber (1978) in conjunction with the isotopic abundances given by Cameron (1980). These are given in Table 3. Elemental abundances for Cl-K and Sc-Mn are also from Cameron (1980) but normalized to the upper limits given by Lezniak and Webber (1978) for these groups. All injection spectra are taken to be proportional to $W^{-2.3}$ where W is total energy per nucleon (Ormes and Freier, 1978). The abundance ratios calculated depend on the injection spectra and primary composition adopted.

We have included the effects of solar modulation on the observed composition by using the "Force Field" solution (Gleeson and Axford, 1968). The modulated spectra $J_i^m(E)$ are obtained from the interstellar spectra $J_i(E)$ at a given kinetic energy per nucleon E by

$$J_i^m(E) \cong \frac{E^2+2E}{(E+\Phi)^2+2(E+\Phi)} \ J_i(E+\Phi) \tag{6}$$

where $\Phi = \phi\frac{Ze}{A}$ is the mean energy loss per nucleon in the heliosphere. We have usually used a deceleration parameter ϕ = 200 MV as being typical of values derived from the data, although the effect of varying ϕ is discussed later.

We also consider the effect on composition of propagation through the atmosphere. For this we solve the slab model equations (equation 3) with initial conditions $J_i^s(E,0) = J_i^m(E)$. For the case of an experiment at a mean slant depth x_A in the atmosphere we take a pathlength distribution $P(x) = \delta(x-x_A)$. In reality, this will be broadened by the finite acceptance solid angles of detectors; but, since this varies from experiment to experiment, we do not consider this effect here. The amount of atmospheric correction necessary can be seen in Figure 2. Here we present results of our calculations of the ratios (Be+B)/C and $(21 \leq Z \leq 25)$/Fe in interstellar space, above the atmosphere (effects of solar modulation with

ϕ = 200 MV) and at various depths in the atmosphere appropriate to balloon-borne experiments. These calculations are for our standard model (to be described in the next section). As can be seen, features in the ratios below about 1 GeV/nuc will be washed out in a few g/cm^2 of atmosphere because of ionization losses.

Interpretation of Be, B, C Composition

The role of the ratio of (Be+B)/C is to determine the mean escape length as outlined in the introduction. Here we present the results of our calculations of the ratio (Be+B)/C as a function of energy for an exponential pathlength distribution. The results are shown in Figure 3 for various mean escape lengths. Here we have used a solar modulation deceleration parameter of ϕ = 200 MV. We also show a survey of the data on this ratio corrected to the top of the atmosphere (in most cases by the original authors). These predictions have been used to derive a mean escape length for each data point and Figure 4 shows the variation of mean escape length with energy obtained in this way. Above 2 GeV/nuc the data are generally interpreted as suggesting that the mean escape length is proportional to E$^{-0.4\pm0.1}$. Below 2 GeV/nuc we find that the mean pathlength is essentially independent of energy at $\sim$7 g/cm^2. This conclusion is based on the data at the lowest energies considered ($\sim$100 MeV/nuc) and is thus sensitive to the amount of solar modulation adopted (ϕ=200 MV) and to the shape of the injection spectrum. The data at $\sim$1 GeV/nuc, where solar modulation is not too important, fix the escape length at about 7 g/cm^2; but at energies around 100 MeV/nuc an escape length as high as 9 g/cm^2 (no solar modulation) or as low as 5 g/cm^2 (ϕ = 400 MV) is also possible. For our "standard model" we therefore adopt

$$\lambda_e(E) = \begin{cases} 7 \text{ g/cm}^2 & E<2 \text{ GeV/nuc} \\ 7\left(\dfrac{E}{2\text{GeV/nuc}}\right)^{-0.4} \text{ g/cm}^2 & E\geq2 \text{ GeV/nuc} \end{cases} \qquad (7)$$

for all species with Z$\geq$2. Predictions of the ratio (Be+B)/C based on this standard model are shown by the dashed curve of Figure 3.

The energy dependence of the mean escape length, above is not expected
to be valid at the highest energies. For example, the mechanism responsible
for this energy dependence would almost certainly break down at energies for
which equation (7) would give a mean escape length less than the thickness of
the galactic disk. Some information about the high energy behaviour may be
obtained from measurements of the anisotropy of cosmic rays. Provided the
streaming of cosmic rays is not much in excess of that necessary to transport
the cosmic ray nuclei from the sources to the escape boundary, then the magnitude
of the expected anisotropy is given by (Kiraly et al., 1979):

$$\xi = t_{DE}/t_{con} \tag{8}$$

where t_{con} is the confinement time of cosmic rays in the galaxy and t_{DE} is the
"direct exit" time, i.e., the escape time of neutral cosmic rays. Since the
confinement time is proportional to escape length, the anistropy would be
inversely proportional to escape length. The measured anisotropy is almost
constant at about 0.05 percent over the energy range 5×10^2 GeV/nucleus to
5×10^4 GeV/nucleus (see the review by Elliot, 1979), and this has been used
by Kiraly et al. (1979a) to infer that the mean escape length is essentially
constant over this energy range. On the other hand, the absence of any
flattening in the cosmic ray proton spectrum up to 2 TeV/nuc suggests that
the energy dependent escape mechanisms continues to at least that energy.
A flattening in the all particle spectrum between 10 and 100 TeV is seen
in air shower spectra. Perhaps this flattening is associated with a change
in the escape mechanism.

The abundances of the elements Li through Ni predicted at various
energies for the standard model are given alongside the source abundances
in table 3. Using this model we can look at other abundance ratios to see
whether they are consistent with the experimental results. In figure 5
we reproduce the survey of data on the ratio $(17 \leq Z \leq 25)/(26 \leq Z \leq 28)$ from Simon

et al. (1980). This is compared with the ratio predicted for the standard model in the figure. The energy dependence of the predicted ratio is in good agreement with the observations, bearing in mind the statistical uncertainties. In particular, we are able to reproduce the observed peak in the abundance ratio at ~ 1 GeV/nuc.

From the variation of the ratio of two "primary" components with energy we can look for variations in the slope of injection spectra between the different elements. A survey of measurements of the Fe/O ratio is given in Figure 6, and it is seen that, despite the large amount of scatter between the data, this ratio increases from ~ 0.8 at 100 MeV/nuc to ~ 1.5 at 100 GeV/nuc. The predicted ratio also increases with energy due to the energy dependence of the relative importance of escape and interaction losses, especially for Fe nuclei. At very high energies, since losses are dominated by escape ($\lambda_e \ll \lambda_{int}$) for both species, the Fe/O ratio approaches the source ratio. Below about 1 GeV/nuc, the ratio is also reduced by ionization losses. These effects are further enhanced for observations made from balloons in the atmosphere. The predicted ratio is shown in Figure 6 for depths of 3, 6 and 9 g/cm^2 in the atmosphere. The scatter in the data is quite large and could arise partly from the use of different atmospheric correction factors by the various authors. Within the uncertainties in the data we do not detect any significant difference between the injection spectra of Fe and O; in this energy range the observed flattening can be explained solely by propagation effects as noted by Cowsik and Wilson (1973).

"Two-zone" or "Nested Leaky Box" Models

The composition of heavy nuclei is particularly sensitive to the shape of the pathlength distribution because the interaction mean free paths of heavy nuclei are much less than the mean escape length (e.g. $\lambda_{int}^{Fe} \approx 2.6$ g/cm^2). Thus if the pathlength distribution were truncated for small pathlengths, then nuclear interactions would have a greater effect in determining the observed composition, resulting in a significantly higher ratio of secondary nuclei to primary nuclei. A similar effect, although not so pronounced, results for the composition of light and medium nuclei, increasing, e.g., the (Be+B)/C ratio observed, and this must be taken into account when deriving the mean escape length from the data for such models.

Cowsik and Wilson (1973, 1975) have shown that "two-zone" or "nested leaky box" models result in a PLD which is the convolution of two exponential distributions. We use the formalism introduced by Simon (1977) to give physical meaning to a parameter which describes the shape of the PLD. The distribution is uniquely defined by two parameters: the mean pathlength in the source region λ_s, and the mean pathlength in the galaxy λ_b (the mean escape length is $\lambda_e = \lambda_s + \lambda_b$, and the ratio λ_s/λ_e determines the shape of the distribution). Pathlength distributions for λ_s/λ_e ranging from 0.0 (pure exponential PLD) to 0.5 (for λ_s/λ_e values greater than 0.5, the shape of the distribution is the same as for $1.0 - \lambda_s/\lambda_e$) are shown in Figure 7 for $\lambda_e = 6$ g/cm^2. We use the ratio λ_s/λ_e here as a convenient parameterization of the shape of the PLD. Once the shape has been determined experimentally, it can be compared with different cosmic ray storage models (Lezniak and Webber, 1979) or source distributions (Owens, 1976).

The variation of the B/C and (Be+B)/C ratios with mean escape length λ_e is given in Figure 8 for various values of λ_s/λ_e. The calculations for this figure were done using the asymptotic cross sections and correspond to energies above 4 GeV/nuc. The cross sections are however almost independent of energy

above 1 GeV. This is fortunate since the (Be+B)/C ratio is best known at around 1-2 GeV/nuc and we shall use this to fix λ_e for different values of λ_s/λ_e. From figure 8 we see that λ_e could vary from 5.2 g/cm^2 ($\lambda_s/\lambda_e = 0.5$) to 7.0 g/cm^2 ($\lambda_s/\lambda_e = 0$), depending on the shape of the PLD, and give the observed (Be+B)/C ratio between 1 and 2 GeV/nuc.

We have calculated the ratio of Iron secondaries ($21 \leq Z \leq 25$) to Fe and (Be+B)/C as a function of energy for two different cases: the standard model ($\lambda_s/\lambda_e = 0$; $\lambda_e = 7$ g/cm^2 below 2 GeV/nuc, $7(E/2)^{-0.4}$ g/cm^2 above 2 GeV/nuc) and for a severly truncated PLD ($\lambda_s/\lambda_e = 0.33$; $\lambda_e = 5.3$ g/cm^2 below 2 GeV/nuc, $5.3(E/2)^{-0.4}$ g/cm^2 above 2 GeV/nuc). The predictions are shown in Figure 9. In the figure, we also show the effect of varying the amount of solar modulation and give results for $\phi = 0$, 200 MV and 400 MV. The predictions for the ($21 \leq Z \leq 25$)/Fe ratio may be compared with a survey of the experimental results shown in the figure. From this comparison, it appears that there is no need to invoke a truncated pathlength distribution to explain the observed ratio. The data are consistent with the predictions for the exponential PLD; however, because of the large amount of scatter between data points, we cannot rule out the possibility of small values of λ_s/λ_e. As can be seen from Figure 9, an increase of 10 percent in the cross sections would reduce these curves by 10 percent but would not alter this conclusion.

A different conclusion has been reached by the Chicago group (Garcia-Munoz et al., 1979). These authors require a PLD of the form exp $(-x/X_o)$ with $X_o = 5$ g/cm^2 of hydrogen (6 g/cm^2) of interstellar material) and truncated with a linear rise between 0 and 1.3 g/cm^2 (hydrogen) to fit both the B/C and Sub-Fe/Fe ratios from 500 MeV/nuc to 1 GeV/nuc. At lower energies they require a lower value of X_o. The discrepancy between this result and our analysis is due mainly to differences in the total (as noted earlier) and spallation cross sections adopted. This underlines the necessity for new cross section measurements. Another difference is in the shape of the injection spectra used. Garcia-Munoz et al. (1979) have adopted $(E + 400 \text{ MeV/nuc})^{-2.6}$ as opposed to our $(E + 938 \text{ MeV/nuc})^{-2.3}$.

This difference is only important at low energies (< 500 MeV/nuc) where ionization losses and solar modulation are important. Their spectrum will clearly be too steep at high energies once energy dependent leakage is taken into account.

Abundance of Individual Iron Secondaries

Using our standard model, we have calculated the expected abundances of the elements Sc, Ti, V, Cr and Mn relative to Fe as a function of energy. The results are shown in Figures 10(a)-(c), where they are compared with the available data. As can be seen, the predicted abundance ratios are in overall reasonable agreement with the data. In particular, the energy dependence of abundance ratios from the preliminary data from the HEAO-3 experiment (Copenhagen-Saclay Collaboration, 1980) is adequately reproduced with the exception of the Mn/Fe ratio which is less steep than that predicted for ^{54}Mn stable against β decay. That this is due to the survival of ^{54}Mn above a few tens of GeV/nuc and almost complete decay below $\sim$ 1 GeV/nuc is shown in Figure 10(a). We also show our prediction for a mean lifetime of ^{54}Mn against β decay of 2×10^6 years (Cassé, 1973) and propagation in a medium of mean density 0.33 atoms/cm^3 (Wiedenbeck and Greiner, 1980). This gives an acceptable fit to the HEAO-3 data although a better fit would result for a shorter decay time or a less dense propagation region.

Because of the large uncertainties attached to the measurements of the spallation cross sections, it is difficult to go further at the present time. Clearly there is interesting structure in these cross sections which should be observable in the abundance ratios of Fe secondaries. Indeed, if a pronounced maximum occurred in a particular cross section at several hundred MeV/nuc, it may be possible to obtain a "direct measurement" of the amount of solar modulation by determining the energy at which the abundance of that species relative to Fe was greatest. The displacement in energy of this peak relative to that in the spallation cross sections would, after correcting for the effect of ionization losses in the interstellar medium, etc., be equal to the mean energy lost in the heliosphere, Φ.

Detailed measurements of the relative abundances of individual Fe-secondary
isotopes may be more suitable for this study. This is because features in
cross sections of individual isotopes are expected to be more pronounced
than in cross sections for the production of a group of isotopes which
contain the superposition of features at different energies. Cosmic ray
data with sufficiently good statistics to measure ratios of individual
nuclei to iron as a function of energy to 3 percent accuracy should soon
be available from the HEAO-3 satellite experiments. This data should be
able to determine λ_s to an accuracy of $\sim$ 0.3 g/cm^2. Before such studies
can be completed, it will be necessary for new and more accurate measurements
of the energy dependence of the spallation cross sections to be made.

Injection Spectra

As noted earlier, the previous interpretation of the observed energy
spectra (Ormes and Freier, 1978) in terms of injection spectra of the form
$W^{-2.3}$, where W is the total energy per nucleon, needs some revision in order
to take into account ionization losses in the interstellar medium and solar
modulation. In figure 11, we give a survey of recent observations of the
energy spectrum of C and Fe. Predictions for the standard model ($W^{-2.3}$
spectrum) with ϕ = 0, 200 MV and 400 MV and for injection spectra proportional
to $R^{-2.3}$ (where R is rigidity) with ϕ = 200 MV are also shown. For the de-
gree of solar modulation usually assumed (i.e. ϕ = 200 MV), the predicted
spectra are seen to be too flat at low energies for the $W^{-2.3}$ model and too
steep for the $R^{-2.3}$ model. It seems that the injection spectra must lie between
these two forms.

Summary

We have calculated the composition of cosmic rays above 100 MeV/nuc
expected for different pathlength distributions and compared our predictions
with the data available. Our calculations include the effects of the energy
dependence of the spallation cross sections, ionization losses, solar modu-
lation and propagation through the atmosphere down to balloon altitudes.

We find that an exponential pathlength distribution is able to account for the ratios of secondary-to-primary nuclei observed in the cosmic radiation from 100 MeV/nuc to several hundred GeV/nuc provided the escape length is about 7 g/cm^2 below 2 GeV/nuc and proportional to $E^{-0.4 \pm 0.1}$ at higher energies. Below 500 MeV/nuc the cosmic ray composition is most sensitive to the shape of the injection spectrum and solar modulation. The shape of the PLD is best measured between 500 MeV/nuc and 2 GeV/nuc and, with the advent of the HEAO-3 results will be limited by our knowledge of both the partial and total cross sections, particularly for interactions of iron nuclei. At energies above ~ 2 GeV/nuc the energy dependence of the escape length dominates. Using our standard model we predict abundances of the individual Fe-secondaries which are consistent with the data available and generally lie about 10 percent above the preliminary HEAO-3 data. A 10 percent increase in the total cross sections would improve the agreement for most of the individual elements, and the general trend of the predicted energy dependence seems to be tracked by the data. An extreme of half the cosmic ray matter being around the source $\lambda_s = 2.6$ g/cm^2 seems to be ruled out by these data; however, any value of $\lambda_s \leqslant 1$ g/cm^2 is possible within the limits of the data, the cross sections, and these calculations.

When better data on Fe-secondary abundances from HEAO-3 become available more refined tests will be possible; however, it will be necessary first to determine the energy dependence of the (Be+B)/C ratio and hence the energy dependence of the escape length with greater precision. In addition, new measurements of the energy dependence of both the total and the spallation cross sections of Fe are vital if the sub-iron cosmic ray data are to be used to more accurately determine the shape of the pathlength distribution.

REFERENCES

Benegas, J. C., Israel, M. H., Klarmann, J., and Maehl, R. C., 1975: Proc. 14th Inst. Cosmic Ray Conf., Munich 1, 251.

Blandford, R. C., and Ostriker, J. P., 1978: Ap. J. 221, L29.

Caldwell, J. H., 1977: Ap. J. 218, 269.

Cameron, A. G. W., 1980: Center for Astrophysics Preprint Series No. 1357.

Cassé, M. 1973, Ap. J. 180, 623.

Copenhagen-Saclay Collaboration, 1980: "Preliminary Results on the Elemental Abundances of Cosmic Ray Nuclei in the Iron Peak" (The HEAO-3 French-Danish Cosmic Ray Spectrometer) presented at the APS and COSPAR meetings.

Cowsik, R., Yash Pal, Tandon, S. N. and Verma, R. P., 1967: Phys. Rev., 158, 1238.

Cowsik, R., and Wilson, L. W., 1973: Proc. 13th Int. Cosmic Ray Conf., Denver 1, 500.

Cowsik, R., and Wilson, L. W., 1975: Proc. 14th Int. Cosmic Ray Conf., Munich 2, 659.

Eichler, D., 1980: Ap. J. 237, 809.

Elliot, H., 1979: Proc. 16th Int. Cosmic Ray Conf., Kyoto, 14, 200.

Fichtel, C. E., and Reames, D. E., 1968: Phys. Rev. 175, 1564.

Fisher, A. J., Hagen, F. A., Maehl, R. C., Ormes, J. F., and Arens, J. F., 1976: Astrophys. J. 205, 938.

Freier, P. S., Young, J., Waddington, C. J., Fickle, R., Gilman, C., and Scarlett, W. R., 1979: Proc. 16th Cosmic Ray Conf. 1, 316.

Garcia-Munoz, M. and Simpson, J. A., 1970: Acta Phys. Acad. Sci. Hungaricae, 29, Suppl. I, 318.

Garcia-Munoz, M., Mason, G. M., and Simpson, J. A., 1977: Proc. 15th Int. Cosmic Ray Conf., Plovdiv 1, 224.

REFERENCES (Cont'd.)

Garcia-Munoz, M., Mason, G. H., Simpson, J. A., and Wefel, J. P., 1977:
Proc. 15th Int. Cosmic Ra' Conf., Plovdiv, 1, 230.

Garcia-Munoz, M. Margolis, S H., Simpson, J. A., and Wefel, J. P., 1979:
Proc. 16th Int. Cosmic Ra' Conf., Kyoto 1, 310 (and erratum: 13, 401)

Gleeson, L. J., and Axford, W. I., 1968: Ap. J. 154, 1011.

Hagen, F. A., 1976: Ph.D. thesis, University of Maryland.

Hagen, F. A., Fisher, A. J., and Ormes, J. F., 1977: Ap. J. 212, 262.

Israel, M. H., Klarmann, J., Love, P. L., and Tueller, J., 1979: Proc.
16th Int. Cosmic Ray Conf , Kyoto 1, 323 (and erratum: 13, 402).

Jokipii, J. R., 1976: Ap. J 208, 900.

Jokipii, J. R., and Higdon, . . C., 1979: Ap. J., 228, 293.

Jones, F. C., 1979: Ap. J. 229, 747.

Julliot, C., Koch, L., and Petrou, N., 1975: Proc. 14th Int. Cosmic Ray
Conf., Munich, 12, 4118.

Juliusson, E., 1974: Ap. J. 191, 331.

Karol, P. J., 1975: Phys. Rev. C. 11, 1203.

Kiraly, P., Kota, J., Osborne, J. L., Stapley, N. R. and Wolfendale, A. W.,
1979: Revista del Nuovo Cimento, 2 (Serie 3), No. 7.

Kiraly, P. Kota, J., Osborne, J. L., Stapley, N. R. and Wolfendale, A. W.,
1979a: Proc. 16th Int. Cosmic Ray Conf., Kyoto, 4, 221.

Lezniak, J. A., 1979: Astrophys. and Space Sci. 63, 279.

Lezniak, J. A., and Webber, W. R., 1978: Ap. J. 223, 676.

Lezniak, J. A., and Webber, W. R., 1979: Astrophys. and Space Sci. 63, 35.

Lund, N., Rasmussen, I. L., Peters, B., Rotenberg, M., and Westergaard, N. J.,
1975: Proc. 14th Int. Cosmic Ray Conf., Munich 1, 263.

MacFall, J.R., Ellsworth, R. W., Ito, A. S. Siohan, F., Streitmatter, R. E.,
Tonwar, S. C., Viswanath, P. R. and Yodh, G. B., 1979: Nucl. Phys. B151, 213.

REFERENCES (Cont'd.)

Maehl, R. C., Ormes, J. F., Fisher, A. J., and Hagen, F. A., 1977: Astrophys. and Space Sci. 47, 163.

Ormes, J. F., and Freier, P. S., 1978: Ap. J. 222, 471

Orth, C. D., Buffington, A., Smoot, G. F. and Mast, T. S., 1978: Ap. J. 226, 1147.

Owens, A. J., 1976 Astrophy s. and Space Sci. 40, 357.

Raisbeck, G. M., 1979: Proc. 16th Int. Cosmic Ray Conf., Kyoto, 14, 146.

Roberts, T. J., Gustafson, H. R., Jones, L. W., Longo, J. F. and Whalley, M. R., 1979: Nucl. Phys., B159, 56.

Scarlett, W. R., Freier, P. S., and Waddington, C. J., 1978: Astrophys. and Space Sci. 59, 301.

Scott, J. S. and Chevalier, R. A., 1975: Ap. J. Lett., 197, L5.

Shapiro, M. M., and Silberberg, R., 1970: Ann. Rev. Nucl. Sci., 20, 323.

Shapiro, M. M., Silberberg, R., and Tsao, C. H., 1973: Proc. 13th Int. Cosmic Ray Conf., Denver 1, 578.

Silberberg, R., and Tsao, C. H., 1973: Ap. J. Suppl. 25, 315.

Silberberg, R., and Tsao, C. H., 1973a: Ap. J. Suppl. 25, 335.

Silberberg, R., and Tsao, C. H., 1977: Ap. J. Suppl. 35, 129.

Silberberg, R., and Tsao, C. H., 1977a: Ap. J. Suppl. 35, 137.

Silberberg, R., and Tsao, C. H., 1977b: Proc. 15th Int. Cosmic Ray Conf., Plovdiv 2, 84.

Simon, M., 1977: Astron. Astrophys. 61, 833.

Simon, M., Spiegelhauer, H., Schmidt, W. K. H., Siohan, F., Ormes, J. F., Balasubrahmanyan, V. K., and Arens, J. F., 1980) Ap. J., 239, 712.

Tsao, C. H., and Silberberg, R., 1979: Proc. 16th Int. Cosmic Ray Conf., Kyoto 2, 202.

Westfall, G. D., Wilson, L. W., Lindstrom, P. J., Crawford, H. J., Greiner, D. E., and Heckman, H. H., 1979: Phys. Rev., C 19, 1309.

Wiedenbeck, M. E. and Greiner, D. E., 1980: Ap. J. Lett. (in press)

FIGURE CAPTIONS

Figure 1. The interstellar ratios (Be+B)/C and (21≤Z≤25)/Fe predicted as a function of energy for the standard model (described later). The effect of neglecting ionization losses and the energy dependence of the spallation cross sections in propagation calculations is illustrated for particles outside the heliosphere (ϕ = 0).

Figure 2. The ratios (Be+B)/C and (21≤Z≤25)/Fe predicted for the standard model outside the heliosphere, above the atmosphere (effect of solar modulation) and at the depths indicated (g/cm^2) in the atmosphere.

Figure 3. The (Be+B)/C ratio predicted for an exponential pathlength distribution for the mean escape lengths (g/cm^2) indicated. The effects of solar modulation with ϕ = 200 MV are included. The experimental data have been corrected for propagation through the atmosphere.

Figure 4. The variation of mean escape length with energy based on our interpretation of the (Be+B)/C ratio and the B/C ratio. The scale at the right of the figure gives the mean escape length for the most extreme two-zone model (discussed later in the text).

Figure 5. A survey of data on the ratio (17≤Z≤25)/(26≤Z≤28) is compared with our prediction for the standard model (solar modulation with ϕ = 200 MV is included). The sumbols are as follows: G, Garcia-Munoz et al., 1977; L, Lezniak and Webber, 1978; J, Juliusson, 1974; O, Orth et al., 1978; Filled circle, Simon et al., 1980.

Figure 6. A survey of data on the Fe/O ratio is compared with our prediction for the standard model. The effect of solar modulation and propagation through 3, 6 and 9 g/cm^2 of atmosphere are indicated.

Figure 7. The shape of the pathlength distribution in the two-zone model for various values of λ_s/λ_b, keeping λ_e fixed.

Figure 8. The variation of B/C and (Be+B) /C at high energies with λ_e for the two-zone model for various values of λ_s/λ_e (the numbers attached to the curves).

Figure 9. The variation with energy of the ratios (Be+B)/C and $(21 \leq Z \leq 25)$/Fe for the standard model and for the two-zone model with $\lambda_s/\lambda_e = 0.33$. Separate curves are given for $\phi = 0$, 200 MV and 400 MV. Symbols for the experimental data on the $(21 \leq Z \leq 25)$/Fe ratio are as follows: M, Maehl et al., 1977; L, Lund et al., 1975; F, Freier et al., 1979; B and G, Benegas et al., 1975; S, Scarlett et al., 1978: Small Diamond, Copenhagen-Saclay Collaboration, 1980, (preliminary HEAO-3 data); Filled circle, Lezniak and Webber, 1978; Large Diamond, Israel et al., 1979; Rectangle, Garcia-Munoz et al., 1979; Dashed Rectangle, Garcia-Munoz et al., 1977.

Figure 10. The predicted and observed abundance of individual Fe-secondary elements: (a) Mn; (b) Cr and Sc; (c) Ti and V.

Figure 11. The measured fluxes of Fe and C are compared with the predictions for the standard model with $\phi = 0$, 200 MV and 400 MV. Also given are predictions for an injection spectrum which is a power law in rigidity. The curves are normalized such that the flux of C at 10 GeV/nuc is 3.2×10^{-2} m^{-2}s^{-1}sr^{-1}(GeV/nuc)$^{-1}$.

TABLE 1

Cosmic Ray Cross Sections (mb) for the Spallation of ^{12}C into Li, Be and B

E(MeV/nuc)	100	251	630	1584	3981
^{6}Li	15.8	15.8	15.3	14.4	14.4
^{7}Li	9.8	11.8	13.0	12.6	12.6
^{7}Be	11.5	12.0	11.7	10.5	10.5
^{9}Be	4.67	5.44	5.47	4.60	4.60
^{10}Be	1.28	2.17	3.06	3.04	3.04
^{10}B	37.5	32.6	27.2	22.4	22.4
^{11}B	82.1	61.5	70.0	62.9	61.4

TABLE 2

Cosmic Ray Cross Sections (mb) for the Spallation of Fe into Sub-Fe Elements

E(MeV/nuc)	100	251	630	1584	3981
Sc	16.8	15.6	29.7	33.3	27.7
Ti	107.1	77.2	118.2	115.1	93.4
V	96.6	53.7	63.6	51.6	42.9
Cr	408.2	183.9	169.9	118.9	104.2
Mn*	271.7	144.0	114.0	94.2	92.8

* ^{54}Mn assumed stable

ORIGINAL PAGE IS
OF POOR QUALITY

TABLE 3

Predicted Cosmic Ray Composition

	SOURCE	INTERSTELLAR ABUNDANCE AT GIVEN ENERGY (MeV/nuc)				
		100	316	1000	3162	10000
Li	0	1.07	1.29	1.59	1.46	0.904
Be*	0	0.618	0.785	0.960	0.843	0.529
B	0	2.04	2.21	2.31	1.86	1.20
C	3.77	9.90	8.81	8.08	7.39	6.32
N	0.302	2.03	2.06	2.11	1.79	1.32
O	4.23	8.67	7.90	7.43	6.98	6.23
F	0.015	0.148	0.174	0.203	0.184	0.133
Ne	0.603	1.36	1.34	1.34	1.27	1.08
Na	0.026	0.170	0.191	0.213	0.201	0.151
Mg	0.892	1.61	1.56	1.55	1.49	1.33
Al	0.113	0.243	0.251	0.277	0.261	0.222
Si	0.872	1.28	1.25	1.28	1.24	1.15
P	0	0.021	0.031	0.054	0.051	0.035
S	0.140	0.230	0.254	0.319	0.307	0.257
Cl	0.001	0.024	0.037	0.066	0.059	0.041
Ar	0.028	0.089	0.115	0.176	0.158	0.118
K	0.001	0.044	0.065	0.014	0.097	0.069
Ca	0.060	0.153	0.183	0.249	0.213	0.171
Sc	0	0.031	0.039	0.057	0.045	0.033
Ti	0.006	0.132	0.151	0.189	0.144	0.111
V	0.001	0.070	0.073	0.079	0.058	0.046
Cr	0.031	0.212	0.199	0.188	0.147	0.127
Mn†	0.023	0.120	0.125	0.119	0.110	0.097
Fe§	1.0	1.0	1.0	1.0	1.0	1.0
Co	0	0.0008	0.0011	0.0014	0.0011	0.0010
Ni	0.042	0.037	0.037	0.038	0.038	0.039

* ^{10}Be assumed stable

† ^{54}Mn assumed stable

§ Normalization

R. J. Protheroe and J. F. Ormes: Code 661, NASA/Goddard Space Fligh Center,

Greenbelt, MD   20771

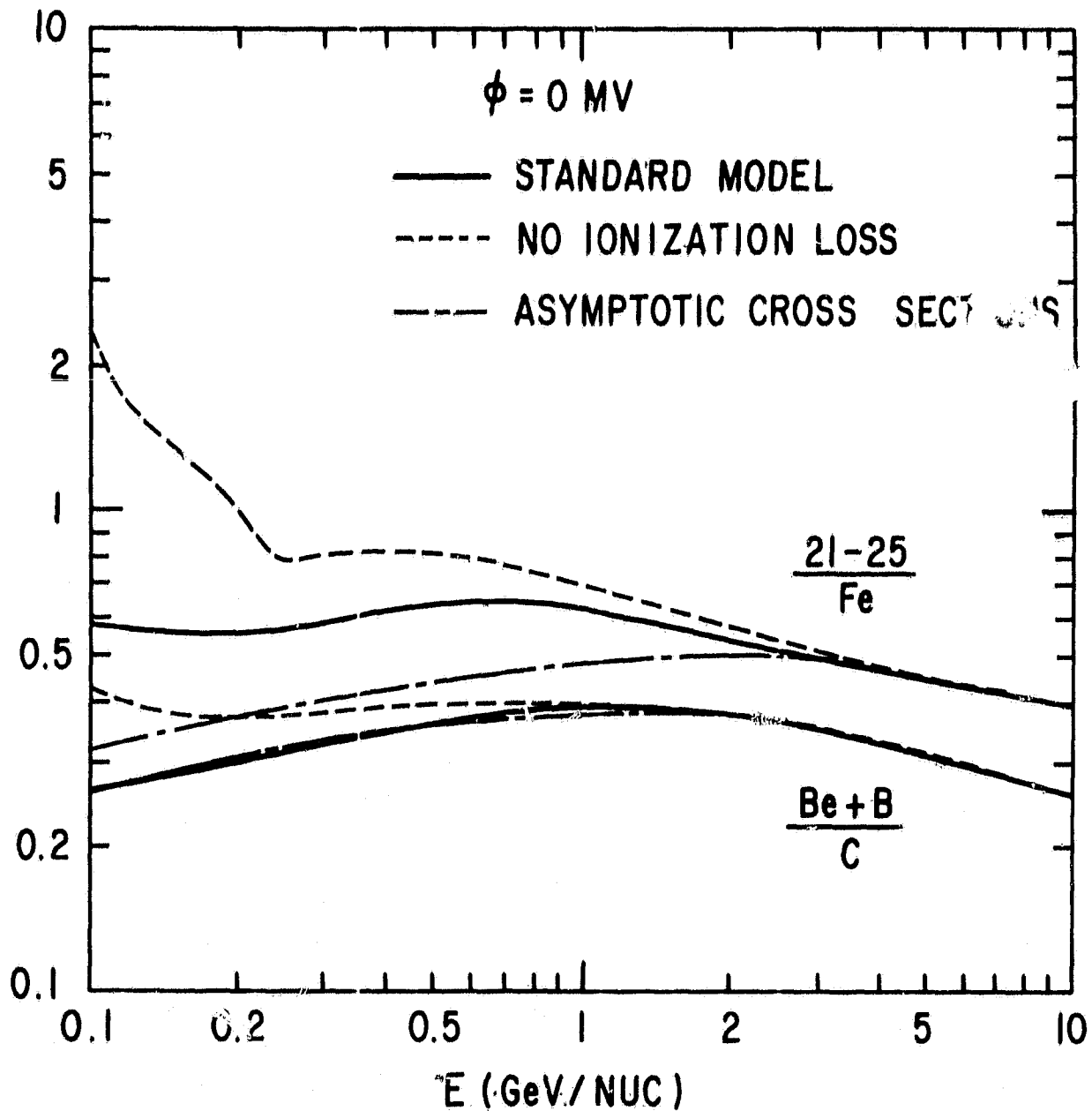G. M. Comstock: Cosmo Science Associates, 21 Erland Road, Stony Brook, NY   11790

Figure 1

Figure 2

Figure 3

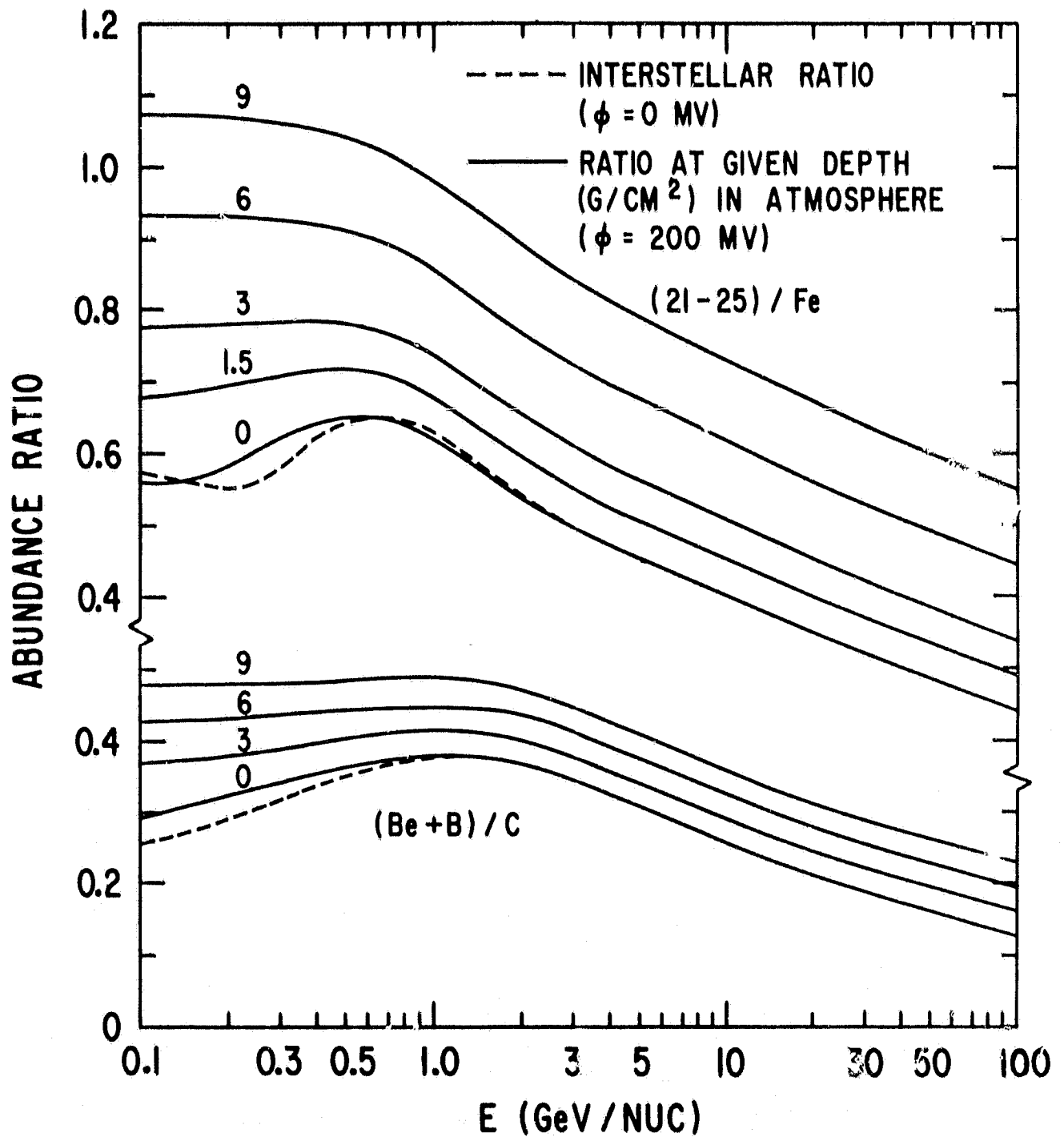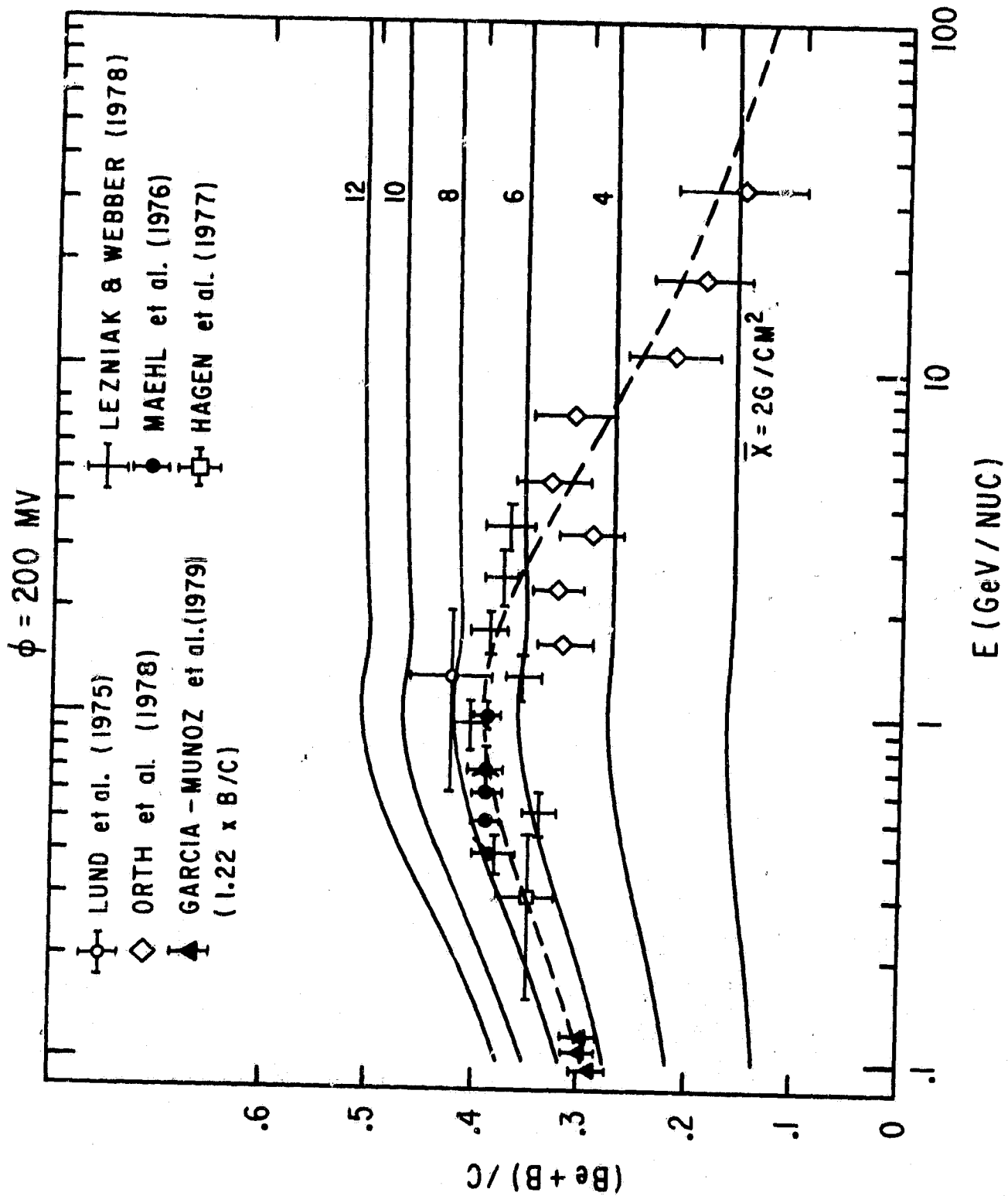Figure 4

ENERGY (GeV/NUCLEON)

λ_e (g/cm^2)

△ GARCIA - MUNOZ et al., 1979
□ HAGEN et al., 1977
L LEZNIAK & WEBBER, 1978
M MAEHL et al., 1977
o ORTH et al., 1978
● SIMON et al., 1980
J JULIUSSON, 1974
C CALDWELL, 1977

Figure 5

INTERSTELLAR RATIO ($\phi = 0$ MV)
RATIO AT GIVEN DEPTH (G/CM^2) IN
ATMOSPHERE ($\phi = 200$ MV)

△ ORTH et al. (1978)
● SIMON et al. (1980)
○ LEZNIAK & WEBBER (1978)
▭ GARCIA-MUNOZ et al. (1979)
◇ JULLIOT et al. (1975)
▢ JULIUSSON (1974)
C CALDWELL (1977)

E (GeV / NUC)

Fe/O

λ_e = AVG. PATHLENGTH = 6 g / cm^2

$\lambda_e = \lambda_s + \lambda_b$

$\int_o^\infty P(x)\,dx = 1$

$\int_o^\infty x\,P(x)\,dx = \lambda_e$

$P(x) = \dfrac{1}{\lambda_b - \lambda_s}\left[e^{-x/\lambda_b} - e^{-x/\lambda_s}\right]$

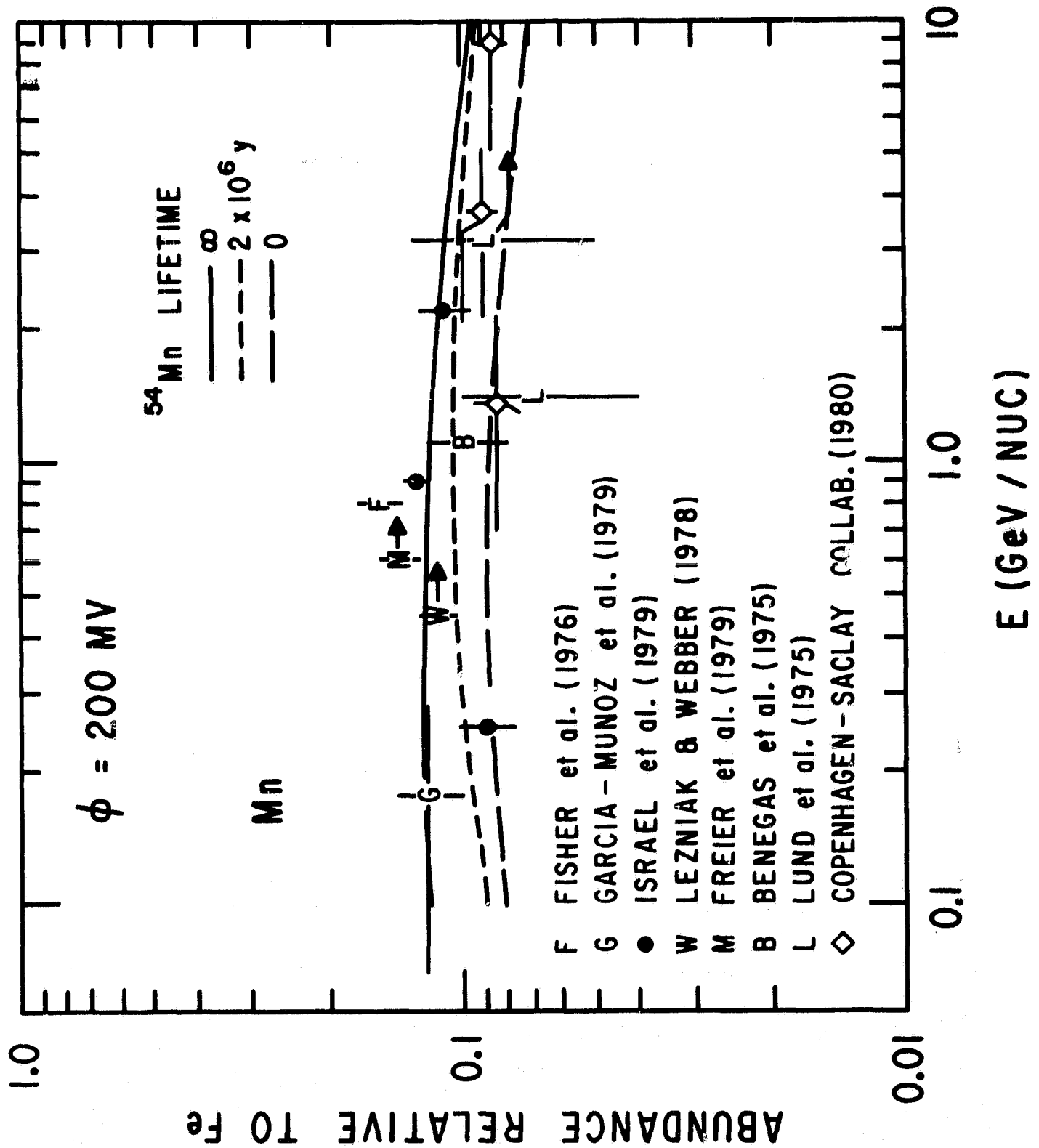$$\frac{B}{C} \& \frac{Be+B}{C} \quad \text{FOR} \quad 0 \le \frac{\lambda_s}{\lambda_e} \le 0.5$$

Figure 8

Figure 9

Figure 10 (a)

Figure 10 (b)

Figure 10 (c)

Figure 11